


Metadata of the chapter that will be visualized online

Chapter Title	Markov Models of Ion Channels	
Copyright Year	2014	
Copyright Holder	Springer Science+Business Media New York	
Author	Family Name	Linaro
	Particle	
	Given Name	Daniele
	Suffix	
	Division	Theoretical Neurobiology and Neuroengineering Laboratory, Department of Biomedical Sciences
	Organization	University of Antwerp
	Address	Campus Drie Eiken T 6.57, Universiteitsplein 1, B-2610, Wilrijk, Belgium
	Email	daniele@tnb.ua.ac.be
Corresponding Author	Family Name	Giugliano
	Particle	
	Given Name	Michele
	Suffix	
	Division	Theoretical Neurobiology and Neuroengineering Laboratory, Department of Biomedical Sciences
	Organization	University of Antwerp
	Address	Campus Drie Eiken T 6.57, Universiteitsplein 1, B-2610, Wilrijk, Belgium
	Division	Department of Computer Science
	Organization	University of Sheffield
	Address	Sheffield, UK
	Division	Brain Mind Institute
	Organization	Swiss Federal Institute of Technology of Lausanne
	Address	Lausanne, Switzerland
	Email	 hele.giugliano@ua.ac.be

1 Markov Models of Ion Channels

2 Daniele Linaro^a and Michele Giugliano^{a,b,c,*}

3 ^aTheoretical Neurobiology and Neuroengineering Laboratory, Department of Biomedical Sciences, University of
 4 Antwerp, Wilrijk, Belgium

5 ^bDepartment of Computer Science, University of Sheffield, Sheffield, UK

6 ^cBrain Mind Institute, Swiss Federal Institute of Technology of Lausanne, Lausanne, Switzerland

7 Synonyms

8 [Kinetic schemes](#); [Markov chains](#)

9 Definition


10 A Markov model is a simplified phenomenological representation of (bio)physical, chemical, or
 11 biological process dynamics, described quantitatively as a set of discrete states and by the ease of
 12 transition through time from one state to another.

13 In chemistry, for instance, a complex reaction can be represented as a kinetic scheme, although
 14 ultimately it occurs from the rearrangement of electrons in the bonds between atoms, according to
 15 the laws of quantum physics. Nonetheless, for most practical purposes, the changes of the reactants'
 16 concentration and their equilibria can be effectively predicted by a reduced kinetic description,
 17 involving simple concepts such as affinity, valence, and reaction rates.

QI 18 In the context of modeling the ionic permeability of a protein channel and the activation of
 19 a (synaptic) membrane receptor, of a transporter, of a second messenger, or of the activity-dependent
 20 short-term synaptic plasticity (Destexhe et al. 1998; Yamada et al. 1998; Tsodyks et al. 1998),
 21 Markov models are widely used and defined as a weighted directed graph, such as those in Figs. 1
 22 and 2. Individual nodes of the graph represent the discrete conformational states that the proteins
 23 tertiary or quaternary structure may assume at a given time, while the edges represent the possible
 24 transitions between states. In addition, a positive (kinetic) coefficient is associated with each edge,
 25 representing the frequency (or rate) of occurrence of the corresponding transition in time.

26 Of course, ion permeation across an excitable biological membrane ultimately depends on
 27 a variety of molecular properties, chemical interactions, and electrostatic effects (Johnston and
 28 Wu 1994; Hille 2001), including the primary structure of protein channels, their subunits' compo-
 29 sition, the charge distribution across their domains, the electrostatic and geometrical properties of
 30 their selectivity filter, their phosphorylation binding sites, the local electric field, and so
 31 on. However, reduced phenomenological descriptions by Markov models allow one to understand
 32 and predict the evolution in time and the equilibrium of each membrane ionic conductance. For such
 33 reasons, Markov models are a versatile tool for modeling the ionic basis of cellular excitability.

34 We also remark that their description, based on a directed graph, captures an important feature of
 35 many – but not all – (bio)physical systems, the Markovian property (Cox and Miller 1965): the
 36 occurrence of a transition from a state to another depends only on the currently occupied state and on

*Email:  ele.giugliano@ua.ac.be

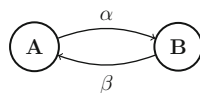


Fig. 1 Markov model of a single ion channel, with two possible states: **A** and **B**. In the graph, the transition probabilities between states per unit of time are indicated by α and β , above each edge

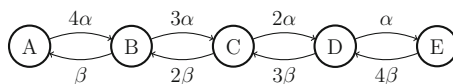


Fig. 2 Markov model of the Hodgkin-Huxley delayed rectifier potassium channel

the transition rates of the edges originating from it, but not on the states occupancy history of the system.

Detailed Description

The most widespread application of Markov models, in the field of computational neuroscience, is the deterministic description of ionic membrane currents across an excitable cell membrane patch (Sterrat et al. 2011). Since these macroscopic currents emerge from the superposition of a large number of microscopic contributions across individual ion channels, we discuss first the dynamics of a single ion channel (Clay and DeFelice 1983; Hille 2001; Colquhoun and Hawkes 2009a). We then introduce the ionic permeability arising from a large population of identical and independent channels, discussing deterministic models of the macroscopic membrane currents. We then briefly discuss numerical methods for the simulation of both stochastic and deterministic versions of Markov models.

Stochastic Description: Single-Channel Dynamics

Let us consider the simplest ion channel: a membrane protein whose three-dimensional conformation has only two possible stable configurations. Therefore, at any given time, the channel can be found only in one of the two states (Fig. 1). We completely neglect the molecular details underlying those stable configurations, as well as the mechanisms of state transition: we phenomenologically describe the system by naming its states with two abstract labels, **A** and **B**. We also assign to each possible transition its corresponding frequency of occurrence: these are assumed to be known from electrophysiological experiments (Conti and Wanke 1975; Colquhoun and Sigworth 2009; Miles et al. 2008; Menon et al. 2009), and they have been indicated as α and β in Fig. 1 and have the unit of the inverse of a time.

The weighted graph summarizes the ion channel dynamics by implying a key underlying hypothesis: the transitions from **A** to **B** or from **B** to **A** occur randomly in time as Poisson point processes (Cox and Miller 1965), with parameters α and β , respectively. This can be rephrased equivalently by specifying the unpredictable character of the intervals between two successive random transitions: these intervals, known as the occupancy lifetimes T , are realizations of continuous random variables, with an exponential probability distribution density $f_T(T)$ (Papoulis and Pillai 2002; Colquhoun and Hawkes 2009a):

$$f_{T_A}(T) = \alpha \exp(-\alpha T), \quad f_{T_B}(T) = \beta \exp(-\beta T) \quad (1)$$

We reconcile our intuition with the style of (graphically) placing α and β above each edge in Fig. 1, by deriving the instantaneous transition probabilities. By definition of probability density, and by evaluating Eq. 1 over a very small interval $T = \Delta t$, it follows that

$$\begin{aligned} \text{Prob}\{\mathbf{A} \rightarrow \mathbf{B} \text{ in } [t; t + \Delta t)\} &= f_{T_A}(\Delta t) \Delta t \approx \alpha \Delta t \\ \text{Prob}\{\mathbf{B} \rightarrow \mathbf{A} \text{ in } [t; t + \Delta t)\} &= f_{T_B}(\Delta t) \Delta t \approx \beta \Delta t \end{aligned}$$

where higher-order infinitesimal terms (e.g., Δt^2 , Δt^3) have been ignored in the Taylor series expansion around $T = 0$, for each exponential function.

These transition probabilities, together with the initial occupancy (probability) conditions, fully describe the dynamics of the ion channel during both transients and steady state. In fact, the time-varying marginal probabilities of occupancy of each state at time t , $P_A(t)$ and $P_B(t)$, can be readily computed from α and β and from the above hypotheses. To this aim, we consider an infinitesimal interval $[t; t + dt)$ and express the probability of observing the ion channel in a state (e.g., \mathbf{A}) at $t + dt$, in terms of the same probability at t . This is equivalent to the conjunction and disjunction of four independent events, expressed by the known quantities: observing the ion channel in \mathbf{A} at t and having no transition $\mathbf{A} \rightarrow \mathbf{B}$ during $[t; t + dt)$ or observing the ion channel in \mathbf{B} at t and having a transition $\mathbf{B} \rightarrow \mathbf{A}$ during the same time interval. Formally, we can write two equations,

$$\begin{aligned} P_A(t + dt) &= P_A(t)(1 - \alpha dt) + P_B(t)\beta dt \\ P_B(t + dt) &= P_B(t)(1 - \beta dt) + P_A(t)\alpha dt \end{aligned}$$

which, in the limit $dt \rightarrow 0$, become a homogeneous system of linear ordinary differential equations, known as the Kolmogorov equations:

$$\begin{aligned} \frac{d}{dt} P_A(t) &= -\alpha P_A(t) + \beta P_B(t) \\ \frac{d}{dt} P_B(t) &= \alpha P_A(t) - \beta P_B(t) \end{aligned}$$

By matrix notation, these equations can be rewritten in compact form as

$$\frac{d}{dt} \mathbf{P} = \mathbf{Q} \mathbf{P} \quad (2)$$

by defining the (column) probability vector \mathbf{P} and the (square) matrix \mathbf{Q} , known as *generator* matrix of the Markov model:

$$\mathbf{P} = \begin{pmatrix} P_A \\ P_B \end{pmatrix}, \quad \mathbf{Q} = \begin{pmatrix} -\alpha & \beta \\ \alpha & -\beta \end{pmatrix}$$

Solving Eq. 2 by analytical or numerical methods (see section “[Deterministic Simulations: Numerical Methods](#)”) gives a complete description of the system, as $\mathbf{P}(t)$ fully reveals statistically its state occupancies at any time t .

Of course, in most cases, a simple two-state kinetic scheme as that of Fig. 1 is not sufficient to model the dynamics of a generic ion channel. Nevertheless, Eq. 2 is a general formulation of the temporal evolution of the statistical occupancy of any Markov model. For kinetic schemes of arbitrary complexity with n states, the probabilities of occupancy at time t are still the solution of the system of n equations, formally Eq. 2, with an appropriate $n \times n$ generator matrix.

For instance, the voltage-gated delayed rectifier potassium channel (Hille 2001) of the Hodgkin-Huxley description of the squid giant axon excitability (Hodgkin and Huxley 1952) is best described by $n = 5$ states and 8 transitions, out of the $n(n - 1) = 20$ theoretically possible (Fig. 2). In this case, the scheme of Fig. 2 has a probability vector \mathbf{P} and a generator matrix \mathbf{Q} , can be defined and derived as in the two-state model, and is given by

$$\mathbf{P} = \begin{pmatrix} P_A \\ P_B \\ P_C \\ P_D \\ P_E \end{pmatrix}, \quad \mathbf{Q} = \begin{pmatrix} -4\alpha & \beta & 0 & 0 & 0 \\ 4\alpha & -(3\alpha + \beta) & 2\beta & 0 & 0 \\ 0 & 3\alpha & -(2\alpha + 2\beta) & 3\beta & 0 \\ 0 & 0 & 2\alpha & -(\alpha + 3\beta) & 4\beta \\ 0 & 0 & 0 & \alpha & -4\beta \end{pmatrix}$$

We further remark that the transition rates, combined together as elements of \mathbf{Q} , can be in general positive functions of time or of any external variable that controls the channel dynamics (e.g., the membrane potential for voltage-gated ion channels or the concentration of a ligand for ligand-gated ion channels). In this case, a closed-form analytical solution of Eq. 2 may not be available. We also note that, by definition, the occupancy probabilities sum to 1 (e.g., $P_A + P_B + \dots + P_E = 1$), so that given a kinetic scheme with n states, only $n - 1$ equations of Eq. 2 are independent. Equivalently, the generator matrix \mathbf{Q} always has at least one null eigenvalue.

We conclude this subsection by adding that no assumption has been made on the reversibility of the transition between any connected pair of states. At the thermodynamical equilibrium, it might be argued that the molecular mechanisms underlying the state transitions must obey a microscopic reversibility principle (Colquhoun and Hawkes 2009a). For the purpose of this review, Markov models have been considered as phenomenological abstract descriptions without accounting for any further microscopic details of channel gating. For instance, strongly asymmetric Markov models may still occur when the microscopic mechanisms are coupled to a source of energy (Colquhoun and Hawkes 2009a). Nonetheless, in the context of experimental identification of the parameters of a Markov model (Conti and Wanke 1975; Colquhoun and Sigworth 2009; Milesu et al. 2008; Menon et al. 2009), imposing constraints for the scheme reversibility might of course be advantageous as it reduces the number of free parameters (Colquhoun and Sigworth 2009).

Stochastic Description: Single-Channel Currents

Relating the ionic currents through a cell membrane patch to single-channel configurations is now mathematically straightforward. For simplicity, we discuss the case in which only one *open* state exists, among the n states of its kinetic scheme. Such a conformational state is the only one to have a nonzero electrical conductance, and we refer to such a value as γ (with typical values ≈ 1 –50 pS). We conventionally rename this state as \mathbf{O} (e.g., corresponding to the state \mathbf{B} in Fig. 1 or to the state \mathbf{E} in Fig. 2), and we associate a (Bernoulli) random variable ξ to it, taking at time t the value 1 with probability $P_O(t)$ or 0 with probability $1 - P_O(t)$: $\xi(t)$ is then a stochastic process of time, with discrete (i.e., binary) values.

We note that, in the context of the matrix notation introduced earlier, $P_O(t)$ can be concisely referred to the solution of Eq. 2, as $P_O(t) = \mathbf{R}\mathbf{P}$, by the definition of an ad hoc (row) vector \mathbf{R} . This

vector has the same number of elements as \mathbf{P} , but all of them are identically zero except for the entry in the position corresponding to the \mathbf{O} state, which is set to 1. For instance, referring to \mathbf{O} as the state \mathbf{B} in the scheme of Fig. 1 implies defining $\mathbf{R} = [0 \ 1]$, while as the state \mathbf{E} in Fig. 2 implies defining $\mathbf{R} = [0 \ 0 \ 0 \ 0 \ 1]$.

Then, the ionic conductance of a single channel is also a Bernoulli random variable for each time t , $g_1(t) = \gamma \xi(t)$, which can take either the value 0 or γ . When N identical and independent ion channels operate in parallel within the same membrane patch, we describe each channel by an identical Markov model and we associate to each of them an independent variable $\xi_k(t)$, $k = 1, 2, 3, \dots, N$, as defined before. The resulting overall conductance of the membrane patch is assumed to be the linear superposition of individual contributions, $g_N(t) = \gamma(\xi_1 + \xi_2 + \dots + \xi_k + \dots + \xi_N)$. $g_N(t)$ is a stochastic process taking discrete random values γ , or 2γ , or $3\gamma, \dots$, or up to a maximal value $\bar{g} = N\gamma$, following a binomial probability distribution (Papoulis and Pillail 2002).

Under the common *ohmic* approximation (Sterrat et al. 2011), the ionic currents of a single channel $I_1(t)$ or of a population of N identical channels $I(t)$ are given by

$$I_1(t) = g_1(t)(E_x - V_m(t)) \quad I(t) = g_N(t)(E_x - V_m(t)) \quad (3)$$

where E_x is the Nernst-Planck equilibrium potential for the ionic species x the channels are selectively permeable to (e.g., $x \in \{Na^+, K^+, Cl^-, Ca^{2+}\}$). Finally, $V_m(t)$ represents the transmembrane electrical potential of the membrane patch.

Introducing a precise motivation for the deterministic formulation of Markov models, discussed next for large populations of identical channels, we report below the ensemble mean and variance of $g_N(t)$ (Conti and Wanke 1975), indicating by $E\{\bullet\}$ the expected value:

$$E\{g_N(t)\} = \bar{g}Po(t) \quad (4)$$

$$Var\{g_N(t)\} = N^{-1}\bar{g}Po(t)(1 - Po(t)). \quad (5)$$

We observe that the variance decreases for increasing values of N . Therefore, by the law of large numbers (Papoulis and Pillail 2002), one may replace the stochastic temporal evolution of $g_N(t)$ by its ensemble mean $E\{g_N(t)\}$ for large N (e.g., in the hundreds or thousands), effectively ignoring the random fluctuations which are intrinsically associated to single-channel permeability. To better clarify this important point, we report the numerical simulations of the open-state dynamics of a population of N Hodgkin-Huxley fast-inactivating sodium ion channels or delayed rectifier potassium ion channels (as in Fig. 2) (Hodgkin and Huxley 1952). Both channel types are described by Markov models, with kinetic rates that change as a function of V_m (Sterrat et al. 2011; Hille 2001). Figure 3 displays as black traces the realizations of the process $g_N(t)$, normalized to its maximal possible value \bar{g} . Such a normalization implies that the fraction of channels in the \mathbf{O} state, out of the total N , is the quantity displayed. These realizations are compared to each others, upon increasing N , ranging from 10 to 1,000 for potassium and from 12 to 1,200 for sodium channels. The thick orange lines in each panel represent instead the expected value of $g_N(t)$ (see Eq. 4) under the same normalization. The generally good agreement between fluctuating realizations and their ensemble averages, for large N (Colquhoun and Hawkes 2009a), illustrates that $E\{g_N(t)\}$ is a good representation of the collective behavior of the channel population, fully disregarding its stochastic properties.

We also remark that from the estimate of the variance of ion currents, recorded experimentally, the number N of channels underlying those currents can be also inferred (Conti and Wanke 1975).

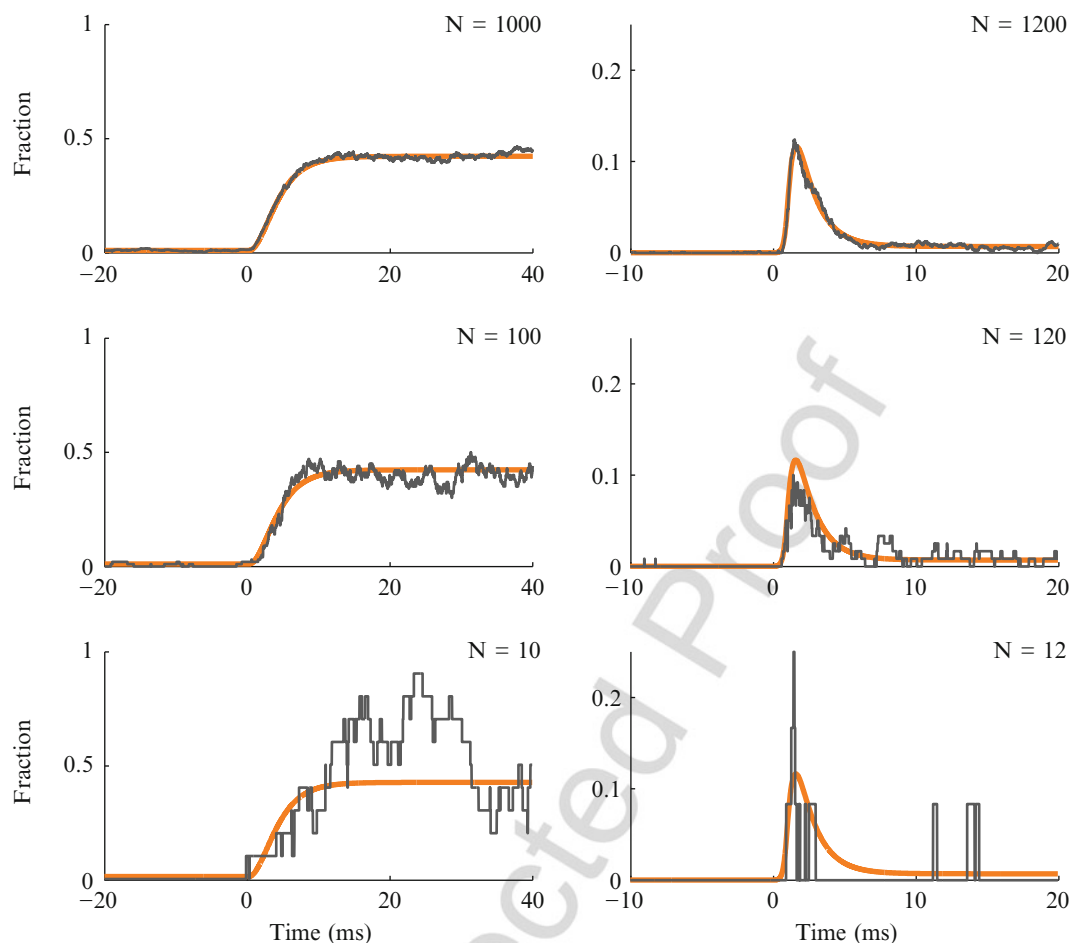


Fig. 3 Numerical stochastic simulations of a step change in the transition rates of potassium (*left column*) and sodium (*right column*) Hodgkin-Huxley voltage-gated channels, obtained for increasing number of identical channels within the same membrane patch. The step is applied as a voltage step, occurring at time $t = 0$ and ranging from -65 to -25 mV. The *black lines* are realizations of the stochastic process underlying channel dynamics (Eq. 3), while the *orange trace* is obtained as Eq. 4, solving numerically Eq. 2

Deterministic Description: Macroscopic Membrane Currents

The previous discussion illustrates that if the fluctuations arising from single-channel (stochastic) dynamics can be neglected (i.e., large N , in the hundreds or thousands), kinetic models and their mathematical formulation by Eq. 2 can still be employed. Equation 4 and Fig. 3 convincingly illustrate the relationship between stochastic and deterministic interpretations, which also corresponds to replacing the probability of an event in a single channel with the relative frequency of its occurrence in a population. In the last case however, the solution of Eq. 2 has a different meaning than the occupancy probabilities: it represents the fractions of state occupancies, across the channels of the population. Conceptually, this implies reinterpreting the Markov models (e.g., Figs. 1 and 2) as first-order kinetic descriptions of the fractions of channels in a given state.

Let us, for instance, consider again the two-state scheme of Fig. 1 and apply the law of mass action: the rate of a transition is proportional to the occupancy fractions of the participating states. This means that the changes in time of the fraction of channels in the state **A** and in the state **B** obey first-order kinetics. Indicating by $a(t)$ and $b(t)$ the fraction of channels in the states **A** and **B**, respectively (i.e., $a(t) + b(t) = 1$), the rate of decrease of $a(t)$ is proportional, via α , to $a(t)$ itself, while the rate of its increase is proportional, via β , to $b(t)$. Formally, this can be written as

$$\begin{aligned}\frac{d}{dt}a(t) &= -\alpha a(t) + \beta b(t) \\ \frac{d}{dt}b(t) &= \alpha a(t) - \beta b(t)\end{aligned}$$

As expected, these equations coincide with the differential equations derived for P_A and P_B : they describe in time the evolution of the ensemble average, i.e., $b(t) \approx E\{g_N(t)/\bar{g}\}$. For the same reason, the evolution of the occupancy fractions in a generic Markov model with n states is given by the solution of the homogeneous system of linear differential equations we already presented:

$$\frac{d}{dt}\mathbf{X}(t) = \mathbf{Q}\mathbf{X}(t) \quad (6)$$

where $\mathbf{X}(t)$ corresponds to $\mathbf{P}(t)$, under the relative frequency interpretation of the probabilities (i.e., as fractions). For the (deterministic) two-state model, the state vector and transition matrices take the form

$$\mathbf{X}(t) = \begin{pmatrix} a \\ b \end{pmatrix} \quad \mathbf{Q} = \begin{pmatrix} -\alpha & \beta \\ \alpha & -\beta \end{pmatrix}$$

Regardless of the conceptual differences, Eqs. 6 and 2 are formally identical and share the exact same generator matrix \mathbf{Q} . As done before, assuming that only one *open* state exists and referring to the fraction of channels in such a state as $o(t)$, the macroscopic membrane current is given by

$$I(t) = \bar{g}o(t)(E_x - V_m(t)), \quad o(t) = \mathbf{R}\mathbf{X}(t).$$

We conclude this section by presenting an example of a “realistic” model, employed in real application to describe deterministically macroscopic membrane currents in neuron models: a Markov model of resurgent sodium channels. This model was originally identified in a series of electrophysiological experiments (Raman and Bean 2001; Khaliq et al. 2003) and is described by the kinetic scheme of Fig. 4, with $n = 13$ states and 34 transitions.

The peculiarity of this kinetic scheme is the presence of a “blocked” state **ob**, to which ion channels quickly transition from the open state. Channels in the **ob** state need to transition again through the open state **o** in order to either inactivate (e.g., **i**₆) or close (e.g., **c**₅), which leads to the resurgent behavior typical of these ion channels. We further note that not all the rate coefficients in Fig. 4 are voltage dependent and that their large diversity gives rise to a variety of time scales, both fast and slow, in the evolution of the state occupancy fractions over time. Figure 5 shows the behavior of a subset of the state variables in response to a step of voltage from -80 to 40 mV and back. The presence of multiple time scales is clearly visible, for instance, in the dynamics of the i_6

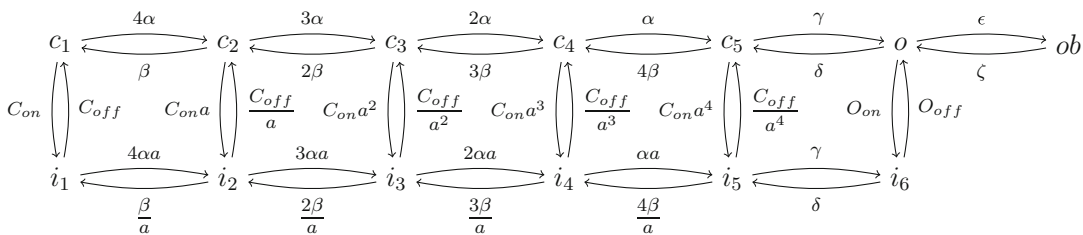


Fig. 4 Kinetic scheme for a resurgent sodium channel

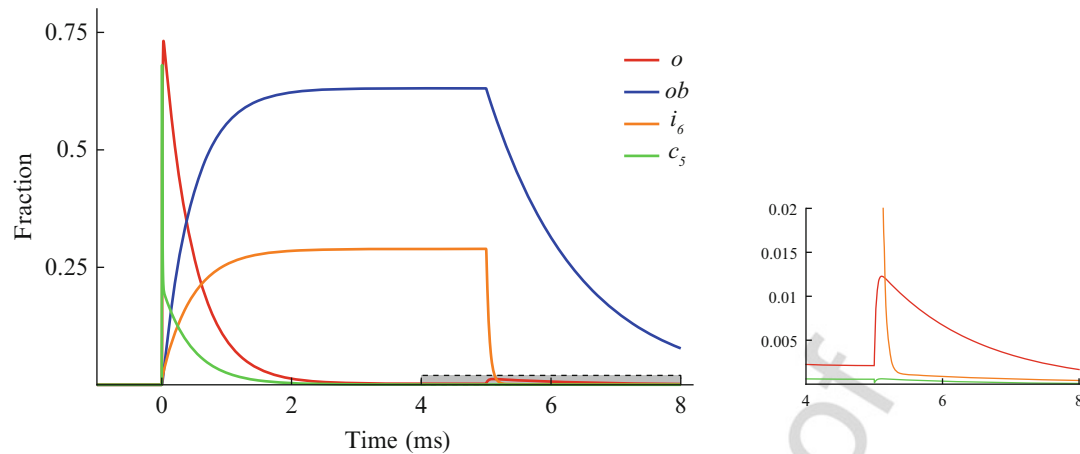


Fig. 5 Time course of a subset of the state occupation fractions, in the resurgent sodium kinetic scheme of Fig. 4, upon a step change of the membrane potential from -80 to 40 mV applied at time $t = 0$ and lasting for 5 ms. The *dashed box* is expanded in the right inset

and c_5 states, while the open state o displays the typical inactivation dynamics of the sodium channels responsible for action potential generation. The inset on the right is an expanded view around the time of the reset of the voltage to -80 mV: the transient increase in the fraction of channels in the open state (red trace) reflects the temporary “flow” of channels occupancies out of the blocked state (blue trace in the main panel) and it gives rise to an additional tail current component.

Stochastic Simulations: Exact Methods

The generation of pseudorandom numbers (Press et al. 2007) is the most important tool for computer simulating random transitions. These routines are today available in any programming language, computing environment, or neural simulator and enable the quick simulation of a variety of deviates (e.g., uniform, Gaussian, binomial, exponential, Bernoulli). For instance, generating a realization of a uniform deviate r in the interval $[0, 1]$ is all that is needed to generate a Bernoulli deviate (e.g., ξ , as introduced earlier). In fact, when repeatedly generating several realizations of r , the number of times its values are below a desired parameter p (e.g., 0.74) is given by p 100 % (e.g., 74 %). It follows that simulating the occurrence of an event with probability, e.g., $P_O(t)$, is as easy as drawing a realization of r and using it within an *if-then* construct, to test for the condition $r \leq P_O(t)$:

- The first simulation method for a Markov model of a single ion channel, implied above, consists in solving (at any time step) Eq. 2 and then refers to its solution $P_O(t) = \mathbf{RP}(t)$, in order to generate Bernoulli (i.e., $g_1(t)$) or binomial (i.e., $g_N(t)$) deviates (Press et al. 2007), needed to update Eq. 3.
- When solving Eq. 2 is computationally intensive, other methods known as Monte Carlo methods can be employed (Mino et al. 2002). The method known as *brute-force* requires to keep track of the current occupied state (for each channel) in the computer memory and consists in simulating the random occurrence of transitions from one state to another of the Markov model, solving no differential equations. This must be performed for each channel and at each time step, updating the current state as the result of the occurrence of a simulated random event. These events are related to the actual transitions of the Markov model, whose probabilities are of course contained in the generator matrix \mathbf{Q} . In fact, a uniform deviate allows one to simulate the random occurrence of a discrete event out of many possible outcomes (e.g., $\{E_1, E_2, E_3\}$), where each has its own

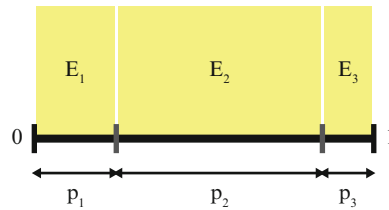


Fig. 6 The random occurrence of an event out of more than two possibilities ($\{E_1, E_2, E_3\}$ in this example), such as the random transitions to one out of more possible target states in a Markov model, can be computer simulated employing a uniform pseudorandom number and testing the interval its realization falls into

probability (e.g., p_1, p_2, p_3). As those probabilities sum to 1, one can graphically arrange these probabilities as (unequal) segments one next to the other, covering the range $[0, 1]$ of r , as in Fig. 6. Upon drawing a realization of r , one can test by multiple *if-then-else* constructs in which of the (three, in this example) intervals the current value of r is located. The equivalent simulated random event that has just been generated is the one corresponding to such an interval, e.g., event E_2 when $p_1 \leq r \leq p_1 + p_2$. For example, considering a single channel described by Fig. 2 and assuming that the currently occupied state is **D**, the algorithm must simulate the occurrence of a discrete event out of three possible outcomes: $\mathbf{D} \rightarrow \mathbf{E}$, $\mathbf{D} \rightarrow \mathbf{C}$, or *stay in D*. All the transition probabilities from **D** must then be listed, $p_1 = \alpha dt$, $p_2 = 3\beta dt$, $p_3 = 1 - (\alpha + 3\beta)$ and conceptually arranged in the range $[0, 1]$ as in Fig. 6. Drawing a realization of r , and computing in which interval r fell, reveals which of the three events occurred and indicates whether and how the currently occupied state has to be updated. Finally, the occupancy of the open state(s) **O** is the link to the actual simulation of the ion current (Eq. 3).

- The *brute-force* method must of course be repeated for each channel and at each time step. For such a reason, it is computationally intensive for moderate to large number of channels N . Most importantly, it requires a large number of deviates to be generated. A more conservative approach is the one of an alternative method that enjoys great popularity: the Gillespie's algorithm (Gillespie 1977). This method involves *event-driven* state occupancy updates, rather than repeating the update procedure at each time step of the simulation. Let us consider a single channel: an exponential deviate T is first generated, simulating the occupancy lifetime of the current state (e.g., as in Eq. 1), with parameter λ . This parameter is the unsigned element on the diagonal of the generator matrix **Q**, corresponding to the current state. The time of the simulation is then asynchronously advanced by T , as opposed to dt . Next, the update of the (newly) occupied state is performed, by drawing again a uniform deviate r and simulating the (conditional) random occurrence of a transition (i.e., excluding by the definition of lifetime the persistence in the current state). For instance, in the example of Fig. 2 and for the currently occupied state **D**, one first obtains a realization of T_D , distributed according to

$$f_{T_D}(T) = \lambda \exp(-\lambda T) \quad \lambda = (\alpha + 3\beta)$$

by equivalently transforming a uniform deviate r as $T = -\log \frac{r}{\lambda}$ (Papoulis and Pillail 2002; Press et al. 2007). Next, another realization of r is drawn and used to randomly simulate the occurrence of one event with two possible outcomes $\mathbf{D} \rightarrow \mathbf{E}$ or $\mathbf{D} \rightarrow \mathbf{C}$, each occurring with (conditional) probabilities $p_1 = \alpha(\alpha + 3\beta)^{-1}dt$ and $p_2 = 3\beta(\alpha + 3\beta)^{-1}dt$. Finally, the occupancy of the open state(s) **O** is the link to the actual simulation of the ion current (Eq. 3). Gillespie's algorithm is still computationally intensive, as the time of occurrence of transitions is inversely proportional to the number of channels. Thus, when a high number of channels are considered, this algorithm takes very

small time steps, which often lead to prohibitive simulation times. On the other hand, for small enough number of channels, these algorithms are very appealing, since they provide an exact simulation of the Markov stochastic kinetics.

This algorithm can be generalized and improved, for simulating a population of channels (Skaugen and Walløe 1979; Chow and White 1996): instead of tracking the state of a single channel, one can describe and simulate how the number of channels in one state must be (randomly) updated by the end of a simulated occupancy lifetime.

Stochastic Simulations: Approximate Methods

An alternative class of algorithms have also been proposed, approximating the discrete-valued stochastic process appearing in Eq. 3 (i.e., $g_N(t)$) as a continuous *diffusion* process (Fox and Lu 1994; Fox 1997; Linaro et al. 2011; Goldwin and Shea-Brown 2011). These algorithms are collectively known as *Langevin methods*, reminiscent of the equation in statistical mechanics describing the random movement of a particle in an aqueous medium, due to collisions with the molecules of the medium (i.e., Brownian motion). Instead of keeping track of the (microscopic) random collisions with every single molecule of the medium, such an equation approximates them by an effective (macroscopic) Gaussian distributed stochastic process, modeled as an external force field in the equation of motion of the particle.

While we point the reader to the cited references for an extended discussion of this approach, we note that in the previous subsections, $g_N(t)$ has been characterized as a binomial distributed stochastic process of time. Under some circumstances (e.g., empirically as $P_{ON} > 30$), a Gaussian deviate well approximates a binomial deviate (Papoulis and Pillail 2002), so that on a first approximation, it should be apparent that $g_N(t)$ in Eq. 3 might be replaced with an ad hoc designed stochastic process with correct mean (Eq. 4) and variance (Eq. 5), among other higher-order statistical properties (Linaro et al. 2011).

This approximation, which in the limit of an infinite number of channels N must coincide with the (deterministic) solution of Eq. 6, has a lower computational load than Monte Carlo methods, and the load is independent on the number of channels, making it most appropriate for moderate to large number of channels and in multicompartmental neuron models.

Deterministic Simulations: Numerical Methods

When the transition rates, and thus the $n \times n$ elements of \mathbf{Q} , are varying in time, the solution of Eq. 6 (and Eq. 2) can only be obtained numerically, for instance, by employing Runge-Kutta method (Press et al. 2007). The update of $\mathbf{X}(t)$ in time occurs by iterating few algebraic equations at each time step of the simulation. However, if \mathbf{Q} has constant elements, at least during each small integration interval dt , a variation of the explicit Euler forward method can be employed,

$$\mathbf{X}(t + dt) \approx e^{\mathbf{Q}(t)dt} \mathbf{X}(t) \quad o(t) = \mathbf{R}\mathbf{X}(t)$$

If the transition rates are constant in time (i.e., or even piecewise constant), the exact solution can also be obtained:

$$\mathbf{X}(t) = \mathbf{X}(0)e^{\mathbf{Q}t} \quad o(t) = \mathbf{R}\mathbf{X}(t)$$

where $\mathbf{X}(0)$ is the known occupancy fraction at the initial time $t = 0$.

The exponential of a matrix appearing in both equations above can be expressed using the spectral expansion $e^{\mathbf{Q}t} = \mathbf{A}^{(1)}e^{s_1t} + \mathbf{A}^{(2)}e^{s_2t} + \dots + \mathbf{A}^{(n)}e^{s_nt}$ (Colquhoun and Hawkes 2009b). The spectral matrices $\mathbf{A}^{(i)}$ are obtained by multiplying the i th column of the matrix \mathbf{M} by the i th row of the inverse matrix \mathbf{M}^{-1} , where \mathbf{M} is the matrix that contains, column-wise, all the eigenvectors of \mathbf{Q} corresponding to the eigenvalue s_i . The parameters s_i , $i = 1 \dots n$, are in fact the eigenvalues of \mathbf{Q} and are the roots of a polynomial of degree n , by definition obtained as the determinant of the matrix $\mathbf{Q} - s\mathbf{I}$, where \mathbf{I} is the identity matrix. For Markov models of ion channels, these roots are in general real and positive and, for simplicity, we also assume that they are all distinct. We also note that as \mathbf{Q} is singular, one eigenvalue is zero and we refer to it as s_1 .

From these considerations, $o(t)$ can be expressed as a simple weighted sum of exponential terms:

$$o(t) = o_\infty + h_2e^{s_2t} + h_3e^{s_3t} + h_4e^{s_4t} + \dots + h_ne^{s_nt}$$

In the previous expression, we have indicated by $o_\infty = \mathbf{R}\mathbf{X}_\infty$ the element corresponding to the open state \mathbf{O} , within the steady-state state vector \mathbf{X}_∞ of Eq. 6. This can be obtained by linear algebraic methods as a solution of the equation $\mathbf{Q}\mathbf{X}_\infty = 0$ or more efficiently as

$$o_\infty = \mathbf{u}(\mathbf{S}^T\mathbf{S})^{-1}\mathbf{R}^T$$

where the matrix \mathbf{S} and its transpose \mathbf{S}^T have been obtained from \mathbf{Q} by addition of an extra (rightmost) column composed of n identical unitary elements, while \mathbf{u} is a (row) vector of n identical unitary elements (Colquhoun and Hawkes 2009b).

Finally, the coefficients h_2, h_3, \dots, h_n are found as the (k th) row in the matrix \mathbf{W} that corresponds to the open state \mathbf{O} within \mathbf{X} (i.e., \mathbf{O} is the k th element of \mathbf{X}). The elements of \mathbf{W} are computed as

$$w_{ij} = \sum_{r=1}^n \mathbf{x}_r(0)\mathbf{a}_{rj}^{(i)}$$

where $\mathbf{x}_r(0)$ is the r th element of $\mathbf{X}(0)$ and $\mathbf{a}_{rj}^{(i)}$ is the generic element of the spectral matrix $\mathbf{A}^{(i)}$.

Independent, Multiple Subunits' Markov Models

We have introduced and described so far a Markov model by means of a single-weighted directed graph. In some cases however, heuristic, experimental, or biophysical considerations may suggest symmetries and constraints on the geometrical arrangement and on the values of the rate coefficients (e.g., compare the scheme of Fig. 2 with the one of Fig. 4). Under these circumstances, a model with several states can be equivalently formulated as a set of Markov models, where each of them has an active and an inactive state (as in Fig. 1). Individual subsystems may not necessarily share identical transition rates and, as a whole, the entire system is said to be in the open state when all its parts are simultaneously activated.

The ionic permeability through a single channel is often attributed to the activation of multiple, independent, protein subunits, which together form the ionic pore through the membrane (Hille 2001). In these cases, following the approach originally proposed by Hodgkin and Huxley (1952), the dynamics of activation of each subunit may be described as a 2-state Markov model, and the resulting membrane permeability is referred to the activations of all subunits at the same time. The single-channel conductance is then readily obtained as a new Bernoulli random variable η , $g_1(t) = \gamma \eta$ obtained multiplying together the elementary independent Bernoulli variables, each

associated with a distinct subunit, e.g., $\eta = \xi^{(1)}(t)\xi^{(2)}(t)\xi^{(3)}(t)\xi^{(4)}(t)$, where each $\xi^{(k)}$ takes the value 1 with probability $P_{\mathbf{B}}(t)$ of the corresponding subunit graph. In the previous example, four independent subunits have been considered, and the channel is in the open state when all four are in an activate state (i.e., all in \mathbf{B}). By describing each subunit by the same kinetic model of Fig. 1 (i.e., same α and β for all four subunits), it is easy to prove that this new description and the one of Fig. 2 are statistically equivalent.

It is possible to rewrite Eq. 3 for the stochastic description of single-channel currents as

$$I_1(t) = \gamma\eta(E_x - V_m(t)) \quad I(t) = \gamma(\eta_1 + \eta_2 + \dots + \eta_k + \dots + \eta_N)(E_x - V_m(t))$$

and for the deterministic description of macroscopic membrane currents as

$$I(t) = \bar{g} b(t)^4 (E_x - V_m(t)).$$

The experimental identification and simulation of these channels is simpler than the full models discussed so far. This is apparent by inspecting the way the analytical expressions of the transient and steady-state solutions of Eq. 2 (and Eq. 6) reduce for multiple subunits, under the hypotheses of time invariance of the rate coefficients already mentioned earlier:

$$P_{\mathbf{A}\infty} = a_{\infty} = \frac{\beta}{\alpha + \beta} \quad P_{\mathbf{B}\infty} = b_{\infty} = \frac{\alpha}{\alpha + \beta}$$

and

$$P_{\mathbf{A}}(t) = (P_{\mathbf{A}}(0) - P_{\mathbf{A}\infty})e^{-(\alpha+\beta)t} + P_{\mathbf{A}\infty}$$

$$P_{\mathbf{B}}(t) = (P_{\mathbf{B}}(0) - P_{\mathbf{B}\infty})e^{-(\alpha+\beta)t} + P_{\mathbf{B}\infty}$$

$$a(t) = (a(0) - a_{\infty})e^{-(\alpha+\beta)t} + a_{\infty}$$

$$b(t) = (b(0) - b_{\infty})e^{-(\alpha+\beta)t} + b_{\infty}$$

Limitations

One of the main assumptions underlying the application of Markov models is the independence of the ion channels in a population. It has been proposed that this assumption may not be always accurate (Undrovinas et al. 1992; Marx et al. 2001) and that coupled gating, i.e., *cooperativity* in transition probabilities, should be instead considered. This was more recently suggested to be hypothesized, at least in specific compartments of neuronal morphologies, such as the axon initial segment, to explain experimental observations. As a consequence, a single-compartmental model has been proposed (Naundorf et al. 2006) that incorporates cooperativity among (groups of) sodium ion channels, where the rate coefficients of each channel depend on the occupancy state of neighboring channels. It was then shown that cooperativity explains some dynamical feature of action potential initiation in cortical neurons, in particular the steep slope of the membrane potential observed both in vitro and in vivo at the onset of the action potential.

However, it is important to note that analogous results have been obtained by employing independent sodium ion channels in a multicompartamental neuron model (Yu et al. 2008).

Another fundamental assumption is that there exists a discrete set of stable configurations (i.e., states) in which an ion channel can reside. An alternative description has been introduced (Liebovitch and Tóth 1990), in which fractals are used to analyze single-channel data, leading to the introduction of a continuum of states, instead of the discrete set commonly used. This makes the transition probabilities depend on time, making the analysis, identification, and simulation more elaborate.

It is not however clear whether either of these alternative formulations realistically captures the biophysics of membrane permeability (Colquhoun and Hawkes 2009a).

Cross-References




- [Compartmental Modeling: Overview](#)
- [Hodgkin-Huxley Model](#)
- [Nernst-Planck Equation](#)
- [Potassium Channels](#)
- [Sodium Channels](#)

References

- Chow C, White J (1996) Spontaneous action potentials due to channel fluctuations. *Biophys J* 71:3013–3021
- Clay J, DeFelice L (1983) Relationship between membrane excitability and single channel open-close kinetics. *Biophys J* 42:151–157
- Colquhoun D, Hawkes A (2009a) The principles of the stochastic interpretation of ion-channel mechanisms. In: Sakmann B, Neher E (eds) *Single-channel recording*, chapter 18, 2nd edn. Springer, New York, pp 397–482
- Colquhoun D, Hawkes A (2009b) A q-matrix cookbook. In: Sakmann B, Neher E (eds) *Single-channel recording*, chapter 20, 2nd edn. Springer, New York
- Colquhoun D, Sigworth F (2009) Fitting and statistical analysis of single-channel records. In: Sakmann B, Neher E (eds) *Single-channel recording*, chapter 19, 2nd edn. Springer, New York, pp 483–586
- Conti F, Wanke E (1975) Channel noise in nerve membranes and lipid bilayers. *Q Rev Biophys* 8:451–506
- Cox D, Miller H (1965) *The theory of stochastic processes*. Chapman and Hall, London
- Destexhe A, Mainen Z, Sejnowski T (1998) Kinetic models of synaptic transmission. In: Segev I, Koch C (eds) *Methods in neuronal modeling*, chapter 1, 2nd edn. MIT Press, Cambridge, pp 1–25
- Fox R (1997) Stochastic versions of the Hodgkin-Huxley equations. *Biophys J* 72:2068–2074
- Fox RF, Yn L (1994) Emergent collective behavior in large numbers of globally coupled independently stochastic ion channels. *Phys Rev E* 49:3421–3431
- Gillespie D (1977) Exact stochastic simulation of coupled chemical reactions. *J Phys Chem* 81:2340–2361
- Goldwin J, Shea-Brown E (2011) The what and where of adding channel noise to the Hodgkin-Huxley equations. *PLoS Comput Biol* 7:e1002247
- Hille B (2001) *Ion channels of excitable membranes*, 3rd edn. Sinauer, Sunderland

- 407 Hodgkin A, Huxley A (1952) A quantitative description of membrane current and its application to
 408 conduction and excitation in nerve. *J Physiol Lond* 117:500–544
- 409 Johnston D, Wu SMS (1994) Foundations of cellular neurophysiology. MIT Press, Cambridge
- 410 Khaliq Z, Gouwens N, Raman I (2003) The contribution of resurgent sodium current to high-
 411 frequency firing in Purkinje neurons: an experimental and modeling study. *J Neurosci*
 412 23:4899–4912
- 413 Liebovitch LS, Tóth TI (1990) Using fractals to understand the opening and closing of ion channels.
 414 *Ann Biomed Eng* 18:177–194
- 415 Linaro D, Storace M, Giugliano M (2011) Accurate and fast simulation of channel noise in
 416 conductance-based model neurons by diffusion approximation. *PLoS Comput Biol* 7:e1001102
- 417 Marx S, Gaburjakova J, Gaburgjakova M, Henrikson C, Ondrias K, Marks AR (2001) Coupled
 418 gating between cardiac calcium release channels (ryanodine receptors). *Circ Res* 88:1151–1158
- 419 Menon V, Spruston N, Kath WL (2009) A state-mutating genetic algorithm to design ion-channel
 420 models. *Proc Natl Acad Sci U S A* 106:16829–16834
- 421 Milesescu LS, Yamanishi T, Ptak K, Mogri MZ, Smith JC (2008) Real-time kinetic modeling of
 422 voltage-gated ion channels using dynamic clamp. *Biophys J* 95:66–87
- 423 Mino H, Rubinstein JT, White JA (2002) Comparison of algorithms for the simulation of action
 424 potentials with stochastic sodium channels. *Ann Biomed Eng* 30:578–587
- 425 Naundorf B, Wolf F, Volgushev M (2006) Unique features of action potential initiation in cortical
 426 neurons. *Nature* 440:1060–1063
- 427 Papoulis A, Pillail SU (2002) Probability, random variables, and stochastic processes, 4th edn.
 428 McGraw-Hill, New York
- 429 Press W, Teukolsky S, Vetterling W, Flannery B (2007) Numerical recipes: the art of scientific
 430 computing. Cambridge University Press, Cambridge/New York
- 431 Raman IM, Bean BP (2001) Inactivation and recovery of sodium currents in cerebellar Purkinje
 432 neurons: evidence for two mechanisms. *Biophys J* 80:729–737
- 433 Skaugen E, Walløe L (1979) Firing behaviour in a stochastic nerve membrane model based upon the
 434 Hodgkin-Huxley equations. *Acta Physiol Scand* 107:343–363
- 435 Sterrat D, Graham B, Gillies A, Willshaw D (2011) Principles of computational modelling in
 436 neuroscience. Cambridge University Press, Cambridge/New York
- 437 Tsodyks M, Pawelzik K, Markram H (1998) Neural networks with dynamic synapses. *Neural*
 438 *Comput* 10:821–835
- 439 Undrovinas A, Fleidervish I, Makielski J (1992) Inward sodium current at resting potentials in single
 440 cardiac myocytes induced by the ischemic metabolite lysophosphatidylcholine. *Circ Res*
 441 71:1231–1241
- 442 Yamada W, Koch C, Adams P (1998) Multiple channels and calcium dynamics. In: Segev I, Koch
 443 C (eds) *Methods in neuronal modeling*, chapter 4. MIT Press, Cambridge, pp 137–170
- 444 Yu Y, Shu Y, McCormick DA (2008) Cortical action potential backpropagation explains spike
 445 threshold variability and rapid-onset kinetics. *J Neurosci Off J Soc Neurosci* 28:7260–7272

Author Queries

Query Refs.	Details Required
	Please check if edit to sentence starting “In the context of modeling...” is okay.
Q2 	Entry title “Potassium Channels” does not match with TOC. Please check.
Q3 	Please check if inserted publisher name for Colquhoun and Sigworth (2009), Colquhoun and Hawkes (2009a, b), Conti and Wanke (1975), Cox and Miller (1965), Destexhe et al. (1998), Hille (2001), Papoulis and Pillail (2002), Press et al. (2007), and Sterrat et al. (2011) are okay.

Uncorrected Proof